Published in final edited form as:

Phys Rev Lett. 2020 September 25; 125(13): 130601. doi:10.1103/PhysRevLett.125.130601.

Minimal Model for Fast Scrambling

Ron Belyansky[*], **Przemyslaw Bienias**, **Yaroslav A. Kharkov**, **Alexey V. Gorshkov**, **Brian Swingle**

Joint Center for Quantum Information and Computer Science, NIST/University of Maryland, College Park, Maryland 20742, USA and Joint Quantum Institute, NIST/University of Maryland, College Park, Maryland 20742, USA

Abstract

We study quantum information scrambling in spin models with both long-range all-to-all and short-range interactions. We argue that a simple global, spatially homogeneous interaction together with local chaotic dynamics is sufficient to give rise to fast scrambling, which describes the spread of quantum information over the entire system in a time that is logarithmic in the system size. This is illustrated in two tractable models: (1) a random circuit with Haar random local unitaries and a global interaction and (2) a classical model of globally coupled nonlinear oscillators. We use exact numerics to provide further evidence by studying the time evolution of an out-of-time-order correlator and entanglement entropy in spin chains of intermediate sizes. Our results pave the way towards experimental investigations of fast scrambling and aspects of quantum gravity with quantum simulators.

Introduction.—

The study of quantum information scrambling has recently attracted significant attention due to its relation to quantum chaos and thermalization of isolated many-body systems [1–3] as well as the dynamics of black holes [4–7]. Scrambling refers to the spread of initially local quantum information over the many-body degrees of freedom of the entire system, rendering it inaccessible to local measurements. Scrambling is also related to the Heisenberg dynamics of local operators, and can be probed via the squared commutator of two local and Hermitian operators W_1, V_r, at positions 1 and r, respectively,

$$\mathscr{C}(r,t) = -\frac{1}{2}\left\langle [W_1(t), V_r]^2 \right\rangle, \tag{1}$$

where $W_1(t)$ is the Heisenberg evolved operator. The growth of the squared commutator corresponds to $W_1(t)$ increasing in size and complexity, leading it to fail to commute with V_r. In a local quantum chaotic system, $\mathscr{C}(r,t)$ typically spreads ballistically, exhibiting rapid growth ahead of the wavefront and saturation behind, at late times [8–10].

Of particular interest are the so-called fast scramblers, systems where $\mathscr{C}(r,t)$ reaches $O(1)$ for all r in a time $t_s \propto \log(N)$, with N being the number of degrees of freedom. Among the best

[*] rbelyans@umd.edu.

known examples are black holes, which are conjectured to be the fastest scramblers in nature [5–7,11], as well as the Sachdev-Ye-Kitaev (SYK) [12,13] model and other related holographic models [14–17].

Recent advances in the development of coherent quantum simulators have enabled the study of out-of-equilibrium dynamics of spin models with controllable interactions [18], making them ideal platforms to experimentally study information scrambling. Several experiments have already been performed [19–24], probing scrambling in either local or nonchaotic systems. The experimental observation of fast scrambling remains challenging however, particularly because few systems are known to be fast scramblers, and those that are, like the SYK model, are highly nontrivial, involving random couplings and many-body interactions. Some recent proposals suggested that spin models with nonlocal interactions can exhibit fast scrambling [25–27], albeit with complicated and inhomogeneous interactions.

In this Letter, we argue that the simplest possible global interaction, together with chaotic dynamics, are sufficient to make a spin model fast scrambling. We consider spin-1/2 chains with Hamiltonians of the form

$$\mathscr{H} = \mathscr{H}_{\text{local}} - \frac{g}{\sqrt{N}} \sum_{i<j} Z_i Z_j, \tag{2}$$

where Z_i is the Pauli z operator acting on site i and $\mathscr{H}_{\text{local}}$ is a Hamiltonian with only local interactions that ensures that the full $\mathscr{H}$ is chaotic. We note that such global interactions are ubiquitous in ultracold atoms in optical cavities [28–32], and also in ion traps [33–36].

We first show that this effect is generic, by studying two models, a random quantum circuit and a classical model, both designed to mimic the universal dynamics of Eq. (2). We then provide numerical evidence for fast scrambling for a particular time-independent quantum Hamiltonian. Finally, we discuss possible experimental realizations.

Random circuit model.—

As a proof of principle, we consider a system of N spin-1/2 sites, with dynamics generated by a random quantum circuit (see Fig. 1) inspired by the Hamiltonian in (Eq. 2). While less physical than the Hamiltonian model, it has the advantage of being exactly solvable while providing intuition about generic many-body chaotic systems with similar features.

The time-evolution operator is $U(t) = (U_{\text{II}} U_{\text{I}})^t$ where a single-time-step update consists of the two layers

$$U_{\text{I}} = \prod_{i=1}^{N} U_{H,i},\ U_{\text{II}} = e^{-i\frac{g}{2\sqrt{N}}\sum_{i<j} Z_i Z_j}, \tag{3}$$

where each $U_{H,i}$ is an independent Haar-random single-site unitary. The two layers in Eq. (3) are motivated by the two terms in Eq. (2), with the Haar-random unitaries replacing $\mathscr{H}_{\text{local}}$.

We are interested in the operator growth of an initially simple operator $\mathcal{O}$. At any point in time, the Heisenberg operator $\mathcal{O}(t) = U^{\dagger}(t)\mathcal{O}U(t)$ can be decomposed as $\mathcal{O}(t) = \sum_{\mathcal{S}} a_{\mathcal{S}}(t)\mathcal{S}$, where $\mathcal{S}$ is a string composed of the Pauli matrices and the identity, forming a basis for SU(2^N). As in random brickwork models [37,38] and random Brownian models [9], the Haar-averaged probabilities $\left\langle a_{\mathcal{S}}^2(t)\right\rangle$, encoding the time evolution of $\mathcal{O}(t)$, themselves obey a linear equation

$$\left\langle a_{\mathcal{S}}^2(t+1)\right\rangle = \sum_{\mathcal{S}'} W_{\mathcal{S},\mathcal{S}'}\left\langle a_{\mathcal{S}'}^2(t)\right\rangle. \tag{4}$$

Here, $W_{\mathcal{S},\mathcal{S}'}$ is a $4^N \times 4^N$ stochastic matrix describing a fictitious Markov process [39,40]. The average probabilities $\left\langle a_{\mathcal{S}}^2(t)\right\rangle$ fully determine the growth of the average of $\mathcal{C}(t)$ in Eq. (1) [see Supplemental Material (SM) [41]]. Because of the Haar unitaries and the simple uniform interaction in Eq. (3), $W_{\mathcal{S},\mathcal{S}'}$ is highly degenerate and only depends on the total weights of the strings $\mathcal{S}$, $\mathcal{S}'$, counting the number of nonidentity operators, i.e., $w(\mathcal{S}) = \sum_i \left(1 - \delta_{\mathcal{S}_i,1}\right)$, and on the number of sites where both $\mathcal{S}$ and $\mathcal{S}'$ are nonidentity, i.e., $v(\mathcal{S},\mathcal{S}') = \sum_i \left(1-\delta_{\mathcal{S}_i,1}\right)\left(1-\delta_{\mathcal{S}',1}\right)$, and is given by (see SM for derivation [41]) [43]

$$\begin{aligned} W(w,w',v) = &\left(\frac{1}{3}\right)^{w+w'} \sum_{k=0}^{v}\binom{v}{k}\sum_{l=0}^{k}\binom{k}{l} \\ &\times\left[\cos^2\left(\frac{2l-k}{\sqrt{N}}g\right)\right]^{N-k-(w+w'-2v)}\left[\sin^2\left(\frac{2l-k}{\sqrt{N}}g\right)\right]^{w+w'-2v}. \end{aligned} \tag{5}$$

If we further assume that $\mathcal{O}$ starts out as a single site operator on site 1, then throughout the evolution, $\left\langle a_{\mathcal{S}}^2(t)\right\rangle$ only depend on the total operator weight w, and the weight on site 1, which we denote by $w_1 \in \{0,1\}$. We thus introduce the operator weight probability h_t at time t,

$$h_t(w,w_1) = \left\langle a_{\mathcal{S}}^2(t)\right\rangle 3^w\binom{N-1}{w-w_1}, \tag{6}$$

which gives the probability of $\mathcal{O}(t)$ having total weight w and weight w_1 on site 1.

The time evolution of $h_t(w, w_1)$ is given by the master equation

$$h_{t+1}(w,w_1) = \sum_{w_1'=0,1}\ \sum_{w'=w_1'}^{N-1+w_1'} \mathcal{R}(w,w_1,w',w_1')h_t(w',w_1'), \tag{7}$$

where the $2N \times 2N$ matrix $\mathcal{R}$ is

$$\mathscr{R}(w, w_1, w', w_1') = 3^w \sum_{m=0}^{\min\{w-w_1,\, w'-w_1'\}} \binom{w'-w_1'}{m} \times \binom{N-1-w'+w_1'}{w-w_1-m} W(w, w', m + w_1 w_1'). \tag{8}$$

The transition matrix $\mathscr{R}$, scaling only linearly with N, allows us to efficiently simulate the dynamics for large system sizes (see Fig. 2).

To proceed analytically, we Taylor expand Eq. (5) to leading order in g, which gives rise to a closed master equation for the total operator weight probability $h_t(w) \equiv h_t(w, 0)\,) + h_t(w, 1)$,

$$\frac{h_{t+1}(w) - h_t(w)}{g^2} = \frac{2w}{9N}(1 - 3N + 2w)h_t(w) + \frac{2w(w+1)}{9N}h_t(w+1) + \frac{N-w+1}{3N}2(w-1)h_t(w-1), \tag{9}$$

which is similar to random Brownian models [9,44] and shows that, at $O(g^2)$, w can change by at most ±1 in a single step. Assuming that $h(w, t)$ varies slowly with respect to $g^2 t$ and w, we can approximate the above equation by a Fokker-Planck equation (rescaling time $\tau = g^2 t$)

$$\partial_\tau h(w, \tau) = -\partial_w[D_1(w)h(w, \tau)] + \partial_w^2[D_2(w)h(w, \tau)], \tag{10}$$

where the drift and diffusion coefficients are [dropping higher order terms $O(1/N, w/N)$]

$$D_1(w) = \frac{2}{3}\left(w - \frac{4w^2}{3N}\right),\ D_2(w) = \frac{w}{3} - \frac{2w^2}{9N}. \tag{11}$$

This equation describes the rapid growth of an initially localized distribution, followed by a broadening and finally saturation (see Fig. 2 and SM [41] for more details). At early time, the $\frac{2}{3}w$ term in the drift coefficient dominates, giving rise to exponential growth of the mean operator weight $\left\langle w(t)\right\rangle \sim e^{2g^2 t/3}$, which agrees with full numerical solution of the master equation, as can be seen in Fig. 2. The mean weight is related to the infinite-temperature squared-commutator in (Eq. 1) (averaged over different circuits) via $\left\langle \mathscr{C}(t)\right\rangle = \frac{4}{3}\left\langle w(t)\right\rangle / N$ [41]. Since $\langle w(t)\rangle$ grows exponentially with time, $\langle w(t)\rangle$ reaches $O(N)$ and $\langle \mathscr{C}(t)\rangle$ reaches $O(1)$ when $t = (3/2g^2)\log(N)$, thus establishing that this model is fast scrambling. Note that the $1/\sqrt{N}$ normalization in (Eqs. 2) and (3) is crucial. Had we chosen instead $1/N (g \to g/\sqrt{N})$, the Lyapunov exponent would have been $2g^2/3N$ and the scrambling time would have been $t \sim N\log(N)$.

Classical model.—

Let us now consider a different setting that also allows us to probe the basic timescales involved, and shows that randomness is not required. A convenient tractable choice is a classical model consisting of globally coupled nonlinear oscillators. Note that the analogs of

out-of-time-order correlators (OTOCs) have been studied in a variety of classical models [26,45–49] and have been shown to capture the scrambling dynamics of quantum models like the SYK model [50–52].

Consider a $2N$-dimensional phase space with coordinates q_r (positions) and p_r (momenta) for $r = 1, \ldots, N$ with canonical structure specified by the Poisson brackets $\{q_r, p_s\}_{\mathrm{PB}} = \delta_{rs}$. The Hamiltonian is $\mathscr{H}_c = K + V_2 + V_4$ where

$$K = \sum_{r=1}^{N} \frac{p_r^2}{2}, \; V_4 = \frac{\Omega_3^2}{4} \sum_{r=1}^{N} q_r^4, \tag{12}$$

$$V_2 = \frac{\Omega_1^2}{2} \sum_{r=1}^{N-1} (q_{r+1} - q_r)^2 + \frac{\Omega_2^2}{2\sqrt{N}} \left(\sum_{r=1}^{N} q_r \right)^2. \tag{13}$$

The timescales for the growth of perturbations under $\mathscr{H}_c$ dynamics may be understood in two stages. First, $K + V_2$ can be solved exactly; this combination of terms provides the nonlocality. The remaining V_4 term renders the dynamics chaotic, provided Ω_3 is large enough. The dynamics of $K + V_2$ causes a localized perturbation to spread to every oscillator with nonlocal amplitude $1/N$ in a time of order $1/N^{1/4}\Omega_2$. Then conventional local chaos can amplify this $1/N$-sized perturbation to order-one size in a time of order $\lambda^{-1} \ln N$, where λ is some typical Lyapunov exponent.

At the quadratic level, the uniform mode, $Q = (1/N) \sum_r q_r$, is decoupled from the remaining modes of the chain. Hence, the propagation of any perturbation is a superposition of the motion due to the local Ω_1 terms and the special dynamics of the uniform mode. Since the local terms cannot induce nonlocal perturbations, we may focus on the dynamics of the uniform mode. The uniform mode's equation of motion is $\left(d^2Q/dt^2\right) = -\sqrt{N}\Omega_2^2 Q$ with solution

$$Q(t) = Q(0)\cos\left(N^{\frac{1}{4}}\Omega_2 t\right) + \frac{\frac{dQ}{dt}(0)}{N^{\frac{1}{4}}\Omega_2}\sin\left(N^{\frac{1}{4}}\Omega_2 t\right). \tag{14}$$

A localized perturbation on site 1 with zero initial time derivative can be written as $\delta\vec{\mathbf{q}}(0) = \epsilon([\hat{\mathbf{e}}_1 - \hat{\mathbf{u}}_0] + \hat{\mathbf{u}}_0)$, where $\hat{\mathbf{u}}_0 = [1, \ldots, 1]^T/N$ represents the uniform mode, $\hat{\mathbf{e}}_1 = [1, 0, \ldots, 0]^T$, and $\hat{\mathbf{e}}_1 - \hat{\mathbf{u}}_0$ is orthogonal to the uniform mode. The orthogonal mode evolves in a local fashion, hence $\delta\vec{\mathbf{q}}(t) = \epsilon\left[\text{ local piece } + \hat{\mathbf{u}}_0 \cos\left(N^{\frac{1}{4}}\Omega_2 t\right)\right]$. For oscillators far from the initial local perturbation, the dynamics is given by

$$\delta q_{r \gg 1}(t) = \frac{\epsilon}{N}\left[\cos\left(N^{\frac{1}{4}}\Omega_2 t\right) - 1\right]. \tag{15}$$

Thus, after a time $\pi/N^{\frac{1}{4}}\Omega_2$, any localized perturbation has spread to distant sites with amplitude ϵ/N.

The inclusion of V_4 renders the equations of motion nonlinear and the system chaotic in at least part of the phase space. We leave a detailed study of the classical chaotic dynamics of this model to the future, but as can be seen in Fig. 3, a numerical solution of the equations of motion displays sensitivity to initial conditions.

The precise protocol is as follows. We compare the dynamics of two configurations, $\vec{\mathbf{q}}^{(1)}$ and $\vec{\mathbf{q}}^{(2)}$, averaged over many initial conditions. The initial condition of configuration one has each oscillator start at rest from a random amplitude drawn uniformly and independently from [−1, 1]. Configuration two is identical to configuration one except that $q_1^{(2)}(0) = q_1^{(1)}(0) + \epsilon$ for $\epsilon = 10^{-5}$. Both configurations are evolved in time and the difference $\Delta q_r(t) = \left|q_r^{(2)}(t) - q_r^{(1)}(t)\right|$ is computed and averaged over 4000 different initial conditions. Figure 3 shows this average of Δq_r for $N = 20$ with $\Omega_1 = 1$, $\Omega_2 = 1$, and $\Omega_3 = 2$. Because the system can generate an ϵ/N-sized perturbation on all sites in a short time, the subsequent uniform exponential growth implies that any local perturbation will become order one on all sites after a time $\sim\lambda^{-1}\log(N/\epsilon)$.

The above analysis corresponds to the classical limit of coupled quantum oscillators where some effective dimensionless Planck's constant vanishes, $\hbar_{\text{eff}} \to 0$. In the opposite limit of large N at fixed $\hbar_{\text{eff}}$, the dynamics of quantum OTOCs can be obtained from the corresponding classical Lyapunov growth up to a timescale of order $\log(1/\hbar_{\text{eff}}) \ll \log N$. At later times, one needs to consider fully quantum local dynamics. If one imagines breaking the system up into local clusters and if each cluster can be viewed as a quantum chaotic system with random-matrix-like energy levels, a dynamical system not unlike the random circuit model above is obtained.

Chaos and level statistics.—

Having established fast scrambling in both the random circuit and the classical model, we now return to the quantum spin model of Eq. (2). We first examine whether such a model is chaotic, which is a necessary condition for it being fast scrambling. For the local Hamiltonian part, we consider the mixed-field Ising chain

$$\mathscr{H}_{\text{local}} = -J\sum_i Z_i Z_{i+1} - h_x\sum_i X_i - h_z\sum_i Z_i\,. \tag{16}$$

A standard approach to identify a transition from integrability to quantum chaos is based on a comparison of energy-level-spacing statistics with Poisson and Wigner-Dyson distributions. Another convenient metric is the average ratio of consecutive level spacings [53] $\langle r\rangle$, where $r = \min(r_n, 1/r_n)$, $r_n = \delta_n/\delta_{n-1}$, $\delta_n = E_n - E_{n-1}$, and E_n are the eigenvalues ordered such that $E_n \geq E_{n-1}$.

As was already suggested in Ref. [54] for a similar model, we find that the longitudinal field is unnecessary, and the full system can have Wigner-Dyson statistics even for $h_z = 0$, in which case $\mathscr{H}_{\text{local}}$ is integrable. The resulting Hamiltonian reads

$$\mathscr{H} = -J\sum_i Z_i Z_{i+1} - h_x \sum_i X_i - \frac{g}{\sqrt{N}} \sum_{i<j} Z_i Z_j . \tag{17}$$

The average adjacent-level-spacing ratio changes from $\langle r \rangle_{\text{Pois}} \approx 0.38$ for Poisson level statistics to $\langle r \rangle_{\text{GOE}} \approx 0.53$ for Wigner-Dyson level statistics in the Gaussian orthogonal ensemble (GOE) [53]. In the vicinity of $g \to 0$, $\langle r \rangle$ (see Fig. 4) shows proximity to Poisson statistics, while, for $|g| \gtrsim 0.25$, the level statistics agree with those of the GOE.

Out-of-time-order correlator and entanglement growth.—

We now study the dynamics of an OTOC and entanglement entropy in the spin chain. We consider the following OTOC:

$$F(r,t) = \Re[\langle Z_1(t) Z_r Z_1(t) Z_r \rangle], \tag{18}$$

which is related to Eq. (1) by $\mathscr{C}(r,t) = 1 - F(r,t)$. The expectation value is evaluated in a Haar-random pure state, which approximates the infinite-temperature OTOC, but enables us to reach larger system sizes [55].

In Fig. 5(a), we show the OTOC for an open chain of $N = 20$ spins for both the local model, governed by $\mathscr{H}_{\text{local}}$ only, and the nonlocal model in (Eq. 17), which includes the global interaction. In the local case, the OTOC spreads ballistically, forming a linear light cone. In contrast, in the nonlocal case, the spreading is superballistic and $F(r \gg 1, t)$ is approximately independent of r, as expected for a fast scrambler. As we discussed in the context of the classical model, a necessary condition for fast scrambling is that, before the onset of exponential growth, the decay of correlations with N should be at most algebraic ($\mathscr{C} \propto N^{-\alpha}$) and not exponential. In Fig. 5(b), we verify that this is the case for the nonlocal model, showing that $\mathscr{C} \propto N^{-1}$ between the two ends of the chain after a fixed time.

Figure 5(c) shows the half-cut entanglement entropy following a quench starting from the $+\hat{\mathbf{y}}$ state for both models. For the local model, the entanglement grows linearly in time before saturating, whereas the nonlocal model shows a significant speed up. Moreover, in the nonlocal model, the growth rate clearly increases with the system size, further supporting our claim.

Experimental realization.—

The Hamiltonian in Eq. (17), and many variations of it, can be experimentally realized in a variety of platforms. A natural realization is with Rydberg dressing of neutral atoms [56–59]. The spin can be encoded in two ground states with one of them dressed to two Rydberg states such that one of the Rydberg states leads to all-to-all interactions and the second to nearest-neighbor interactions. Other similar spin models can be realized with cavity-QED

setups, using photon-mediated all-to-all interactions [28,31,60,61] of the XX or XXZ-Heisenberg form [25,27] together with nearest-neighbor interactions achieved by Rydberg dressing one of the grounds states [62,63]. Other possibilities include a chain of coupled superconducting qubits, with all-to-all flip-flop interactions mediated via a common bus [64–66] or trapped ions [33–36,67].

Conclusion and outlook.—

In this Letter, we argued that a single global interaction together with local chaotic dynamics is sufficient to give rise to fast scrambling. While fast scrambling is intrinsically difficult to study numerically, our numerical evidence, together with the semiclassical analysis and the exactly solvable random circuit, provide a compelling argument in favor of our claim. Our models do not require disordered or inhomogeneous couplings and are within reach of current state-of-the-art quantum simulators. Thus, an experimental implementation of the spin model could test our claims on much larger system sizes, something that may very well be impossible to do on a classical computer. This can pave the way towards experimental investigations of aspects of quantum gravity.

Future theoretical work may include a more systematic analysis of the N dependence of various timescales, e.g., for entanglement growth, and of the behavior of the OTOC at low temperatures. It is also interesting to investigate whether similar conclusions can be reached without perfectly uniform global interactions, for example with power-law decaying interactions.

We thank A. Lucas for useful discussions, especially regarding the normalization of the global interactions. We acknowledge discussions with S. Xu at early stages of this work and P. Titum for pointing out the Hamiltonian [Eq. (17)] to us. R. B., P. B., Y. A. K., and A. V. G. acknowledge funding by the NSF PFCQC program, DoE ASCR Quantum Testbed Pathfinder program (Award No. DE-SC0019040), DoE BES Award No. DESC0019449, DoE ASCR Accelerated Research in Quantum Computing program (Award No. DESC0020312), AFOSR Multidisciplinary University Research Initiative (MURI), AFOSR, ARO MURI, NSF PFC at JQI, and ARL CDQI. R. B. acknowledges support of NSERC and FRQNT of Canada. B. G. S. is supported in part by the U.S. Department of Energy, Office of Science, Office of High Energy Physics QuantISED Award desc0019380.

Note added.—

We would like to draw the reader’s attention to two related parallel works which appeared recently: by Li, Choudhury, and Liu [68], on fast scrambling with similar spin models; and by Yin and Lucas [69], on lower bounds of the scrambling time in similar spin models.

Supplementary Material

Refer to Web version on PubMed Central for supplementary material.

References

[1]. Deutsch JM, Quantum statistical mechanics in a closed system, Phys. Rev. A 43, 2046 (1991). [PubMed: 9905246]

[2]. Srednicki M, Chaos and quantum thermalization, Phys. Rev. E 50, 888 (1994).

[3]. Rigol M, Dunjko V, and Olshanii M, Thermalization and its mechanism for generic isolated quantum systems, Nature (London) 452, 854 (2008). [PubMed: 18421349]

[4]. Hayden P and Preskill J, Black holes as mirrors: Quantum information in random subsystems, J. High Energy Phys 09 (2007) 120.

[5]. Lashkari N, Stanford D, Hastings M, Osborne T, and Hayden P, Towards the fast scrambling conjecture, J. High Energy Phys 4 (2013) 022.

[6]. Shenker SH and Stanford D, Black holes and the butterfly effect, J. High Energy Phys 3 (2014) 067.

[7]. Maldacena J, Shenker SH, and Stanford D, A bound on chaos, J. High Energy Phys 8 (2016) 106.

[8]. Patel AA, Chowdhury D, Sachdev S, and Swingle B, Quantum Butterfly Effect in Weakly Interacting Diffusive Metals, Phys. Rev. X 7, 031047 (2017).

[9]. Xu S and Swingle B, Locality, Quantum Fluctuations, and Scrambling, Phys. Rev. X 9, 031048 (2019).

[10]. Xu S and Swingle B, Accessing scrambling using matrix product operators, Nat. Phys 16, 199 (2020).

[11]. Sekino Y and Susskind L, Fast scramblers, J. High Energy Phys 10 (2008) 065.

[12]. Sachdev S and Ye J, Gapless Spin-Fluid Ground State in a Random Quantum Heisenberg Magnet, Phys. Rev. Lett 70, 3339 (1993). [PubMed: 10053843]

[13]. Kitaev A, A simple model of quantum holography, in KITP Program: Entanglement in Strongly-Correlated Quantum Matter (2015), http://online.kitp.ucsb.edu/online/entangled15/kitaev/.

[14]. Danshita I, Hanada M, and Tezuka M, Creating and probing the Sachdev-Ye-Kitaev model with ultracold gases: Towards experimental studies of quantum gravity, Prog. Theor. Exp. Phys 2017, 83 (2017).

[15]. Chen A, Ilan R, de Juan F, Pikulin DI, and Franz M, Quantum Holography in a Graphene Flake with an Irregular Boundary, Phys. Rev. Lett 121, 036403 (2018). [PubMed: 30085787]

[16]. Chew A, Essin A, and Alicea J, Approximating the Sachdev-Ye-Kitaev model with Majorana wires, Phys. Rev. B 96, 121119(R) (2017).

[17]. Gu Y, Qi X-L, and Stanford D, Local criticality, diffusion and chaos in generalized Sachdev-Ye-Kitaev models, J. High Energy Phys 05 (2017) 125.

[18]. Cirac JI and Zoller P, Goals and opportunities in quantum simulation, Nat. Phys 8, 264 (2012).

[19]. Li J, Fan R, Wang H, Ye B, Zeng B, Zhai H, Peng X, and Du J, Measuring Out-of-Time-Order Correlators on a Nuclear Magnetic Resonance Quantum Simulator, Phys. Rev. X 7, 031011 (2017).

[20]. Gärttner M, Bohnet JG, Safavi-Naini A, Wall ML, Bollinger JJ, and Rey AM, Measuring out-of-time-order correlations and multiple quantum spectra in a trapped-ion quantum magnet, Nat. Phys 13, 781 (2017).

[21]. Wei KX, Ramanathan C, and Cappellaro P, Exploring Localization in Nuclear Spin Chains, Phys. Rev. Lett 120, 070501 (2018). [PubMed: 29542978]

[22]. Landsman KA, Figgatt C, Schuster T, Linke NM, Yoshida B, Yao NY, and Monroe C, Verified quantum information scrambling, Nature (London) 567, 61 (2019). [PubMed: 30842638]

[23]. Joshi MK, Elben A, Vermersch B, Brydges T, Maier C, Zoller P, Blatt R, and Roos CF, Quantum information scrambling in a trapped-ion quantum simulator with tunable range interactions, Phys. Rev. Lett 124, 240505 (2020). [PubMed: 32639800]

[24]. Blok MS, Ramasesh VV, Schuster T, O'Brien K, Kreikebaum JM, Dahlen D, Morvan A, Yoshida B, Yao NY, and Siddiqi I, Quantum Information Scrambling in a Superconducting Qutrit Processor, arXiv:2003.03307.

[25]. Swingle B, Bentsen G, Schleier-Smith M, and Hayden P, Measuring the scrambling of quantum information, Phys. Rev. A 94, 040302(R) (2016).

[26]. Marino J and Rey AM, Cavity-QED simulator of slow and fast scrambling, Phys. Rev. A 99, 051803(R) (2019).

[27]. Bentsen G, Hashizume T, Buyskikh AS, Davis EJ, Daley AJ, Gubser SS, and Schleier-Smith M, Treelike Interactions and Fast Scrambling with Cold Atoms, Phys. Rev. Lett 123, 130601 (2019). [PubMed: 31697527]

[28]. Sørensen AS and Mølmer K, Entangling atoms in bad cavities, Phys. Rev. A 66, 022314 (2002).

[29]. Chaudhury S, Merkel S, Herr T, Silberfarb A, Deutsch IH, and Jessen PS, Quantum Control of the Hyperfine Spin of a Cs Atom Ensemble, Phys. Rev. Lett 99, 163002 (2007). [PubMed: 17995247]

[30]. Fernholz T, Krauter H, Jensen K, Sherson JF, Sørensen AS, and Polzik ES, Spin Squeezing of Atomic Ensembles Via Nuclear-Electronic Spin Entanglement, Phys. Rev. Lett 101, 073601 (2008). [PubMed: 18764532]

[31]. Leroux ID, Schleier-Smith MH, and Vuletić V, Implementation of Cavity Squeezing of a Collective Atomic Spin, Phys. Rev. Lett 104, 073602 (2010). [PubMed: 20366881]

[32]. Schleier-Smith MH, Leroux ID, and Vuletić V, Squeezing the collective spin of a dilute atomic ensemble by cavity feedback, Phys. Rev. A 81, 021804(R) (2010).

[33]. Sawyer BC, Britton JW, Keith AC, Wang C-CJ, Freericks JK, Uys H, Biercuk MJ, and Bollinger JJ, Spectroscopy and Thermometry of Drumhead Modes in a Mesoscopic Trapped-Ion Crystal Using Entanglement, Phys. Rev. Lett 108, 213003 (2012). [PubMed: 23003249]

[34]. Britton JW, Sawyer BC, Keith AC, Wang C-CJ, Freericks JK, Uys H, Biercuk MJ, and Bollinger JJ, Engineered two-dimensional Ising interactions in a trapped-ion quantum simulator with hundreds of spins, Nature (London) 484, 489 (2012). [PubMed: 22538611]

[35]. Wang C-CJ, Keith AC, and Freericks JK, Phonon-mediated quantum spin simulator employing a planar ionic crystal in a Penning trap, Phys. Rev. A 87, 013422 (2013).

[36]. Bohnet JG, Sawyer BC, Britton JW, Wall ML, Rey AM, Foss-Feig M, and Bollinger JJ, Quantum spin dynamics and entanglement generation with hundreds of trapped ions, Science 352, 1297 (2016). [PubMed: 27284189]

[37]. Nahum A, Vijay S, and Haah J, Operator Spreading in Random Unitary Circuits, Phys. Rev. X 8, 021014 (2018).

[38]. von Keyserlingk CW, Rakovszky T, Pollmann F, and Sondhi SL, Operator Hydrodynamics, OTOCs, and Entanglement Growth in Systems Without Conservation Laws, Phys. Rev. X 8, 021013 (2018).

[39]. Dahlsten OCO, Oliveira R, and Plenio MB, The emergence of typical entanglement in two-party random processes, J. Phys. A 40, 8081 (2007).

[40]. Žnidarič M, Exact convergence times for generation of random bipartite entanglement, Phys. Rev. A 78, 032324 (2008).

[41]. See Supplemental Material at http://link.aps.org/supplemental/10.1103/PhysRevLett.125.130601 for additional details concerning the random circuit including the derivation, which includes Ref. [42].

[42]. Zhang L, Matrix integrals over unitary groups: An application of Schur-Weyl duality, arXiv:1408.3782.

[43]. The term with $2l = k$, $w + w' - 2v = 0$ is assumed to be $0^0 = 1$. See Ref. [41].

[44]. Zhou T and Chen X, Operator dynamics in a Brownian quantum circuit, Phys. Rev. E 99, 052212 (2019). [PubMed: 31212479]

[45]. Rozenbaum EB, Ganeshan S, and Galitski V, Lyapunov Exponent and Out-of-Time-Ordered Correlator's Growth Rate in a Chaotic System, Phys. Rev. Lett 118, 086801 (2017). [PubMed: 28282154]

[46]. Bilitewski T, Bhattacharjee S, and Moessner R, Temperature Dependence of the Butterfly Effect in a Classical Many-Body System, Phys. Rev. Lett 121, 250602 (2018). [PubMed: 30608848]

[47]. Chávez-Carlos J, López-del Carpio B, Bastarrachea-Magnani MA, Stránský P, Lerma-Hernández S, Santos LF, and Hirsch JG, Quantum and Classical Lyapunov Exponents in Atom-Field Interaction Systems, Phys. Rev. Lett 122, 024101 (2019). [PubMed: 30720302]

[48]. Jalabert RA, García-Mata I, and Wisniacki DA, Semiclassical theory of out-of-time-order correlators for low-dimensional classically chaotic systems, Phys. Rev. E 98, 062218 (2018).

[49]. Yan B, Cincio L, and Zurek WH, Information Scrambling and Loschmidt Echo, Phys. Rev. Lett 124, 160603 (2020). [PubMed: 32383929]

[50]. Kurchan J, Quantum bound to chaos and the semiclassical limit, J. Stat. Phys 171, 965 (2018).

[51]. Schmitt M, Sels D, Kehrein S, and Polkovnikov A, Semiclassical echo dynamics in the Sachdev-Ye-Kitaev model, Phys. Rev. B 99, 134301 (2019).

[52]. Scaffidi T and Altman E, Chaos in a classical limit of the Sachdev-Ye-Kitaev model, Phys. Rev. B 100, 155128 (2019).

[53]. Atas YY, Bogomolny E, Giraud O, and Roux G, Distribution of the Ratio of Consecutive Level Spacings in Random Matrix Ensembles, Phys. Rev. Lett 110, 084101 (2013). [PubMed: 23473149]

[54]. Lerose A, Marino J, Žunkovič B, Gambassi A, and Silva A, Chaotic Dynamical Ferromagnetic Phase Induced by Nonequilibrium Quantum Fluctuations, Phys. Rev. Lett 120, 130603 (2018). [PubMed: 29694194]

[55]. Luitz DJ and Lev YB, Information propagation in isolated quantum systems, Phys. Rev. B 96, 020406(R) (2017).

[56]. Honer J, Weimer H, Pfau T, and Büchler HP, Collective Many-Body Interaction in Rydberg Dressed Atoms, Phys. Rev. Lett 105, 160404 (2010). [PubMed: 21230953]

[57]. Graß T, Bienias P, Gullans MJ, Lundgren R, Maciejko J, and Gorshkov AV, Fractional Quantum Hall Phases of Bosons with Tunable Interactions: From the Laughlin Liquid to a Fractional Wigner Crystal, Phys. Rev. Lett 121, 253403 (2018). [PubMed: 30608850]

[58]. Pupillo G, Micheli A, Boninsegni M, Lesanovsky I, and Zoller P, Strongly Correlated Gases of Rydberg-Dressed Atoms: Quantum and Classical Dynamics, Phys. Rev. Lett 104, 223002 (2010). [PubMed: 20867164]

[59]. Glaetzle AW, Nath R, Zhao B, Pupillo G, and Zoller P, Driven-dissipative dynamics of a strongly interacting Rydberg gas, Phys. Rev. A 86, 043403 (2012).

[60]. Gopalakrishnan S, Lev BL, and Goldbart PM, Frustration and Glassiness in Spin Models with Cavity-Mediated Interactions, Phys. Rev. Lett 107, 277201 (2011). [PubMed: 22243326]

[61]. Strack P and Sachdev S, Dicke Quantum Spin Glass of Atoms and Photons, Phys. Rev. Lett 107, 277202 (2011). [PubMed: 22243327]

[62]. Gelhausen J, Buchhold M, Rosch A, and Strack P, Quantum-optical magnets with competing short- and long-range interactions: Rydberg-dressed spin lattice in an optical cavity, SciPost Phys. 1, 004 (2016).

[63]. Zhu B, Marino J, Yao NY, Lukin MD, and Demler EA, Dicke time crystals in driven-dissipative quantum many-body systems, New J. Phys 21, 073028 (2019).

[64]. Majer J, Chow JM, Gambetta JM, Koch J, Johnson BR, Schreier JA, Frunzio L, Schuster DI, Houck AA, Wallraff A, Blais A, Devoret MH, Girvin SM, and Schoelkopf RJ, Coupling superconducting qubits via a cavity bus, Nature (London) 449, 443 (2007). [PubMed: 17898763]

[65]. Zhu G, Hafezi M, and Grover T, Measurement of many-body chaos using a quantum clock, Phys. Rev. A 94, 062329 (2016).

[66]. Onodera T, Ng E, and McMahon PL, A quantum annealer with fully programmable all-to-all coupling via Floquet engineering, npj Quantum Inf. 6, 48 (2020).

[67]. Genway S, Li W, Ates C, Lanyon BP, and Lesanovsky I, Generalized Dicke Nonequilibrium Dynamics in Trapped Ions, Phys. Rev. Lett 112, 023603 (2014). [PubMed: 24484012]

[68]. Li Z, Choudhury S, and Liu WV, Fast scrambling without appealing to holographic duality, arXiv:2004.11269.

[69]. Yin C and Lucas A, Bound on quantum scrambling with all-to-all interactions, Phys. Rev. A 102, 022402 (2020).

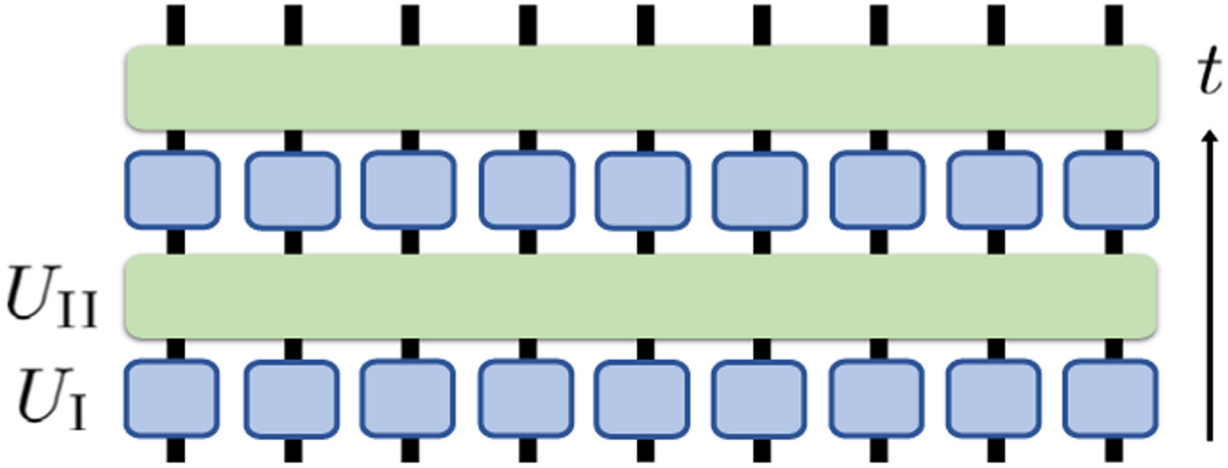

FIG. 1.

Diagram of the random circuit. As given in Eq. (3), each blue square is an independent Haar-random unitary $U_{H,i}$ acting on site i, and the green rectangle is the global interaction U_{II}.

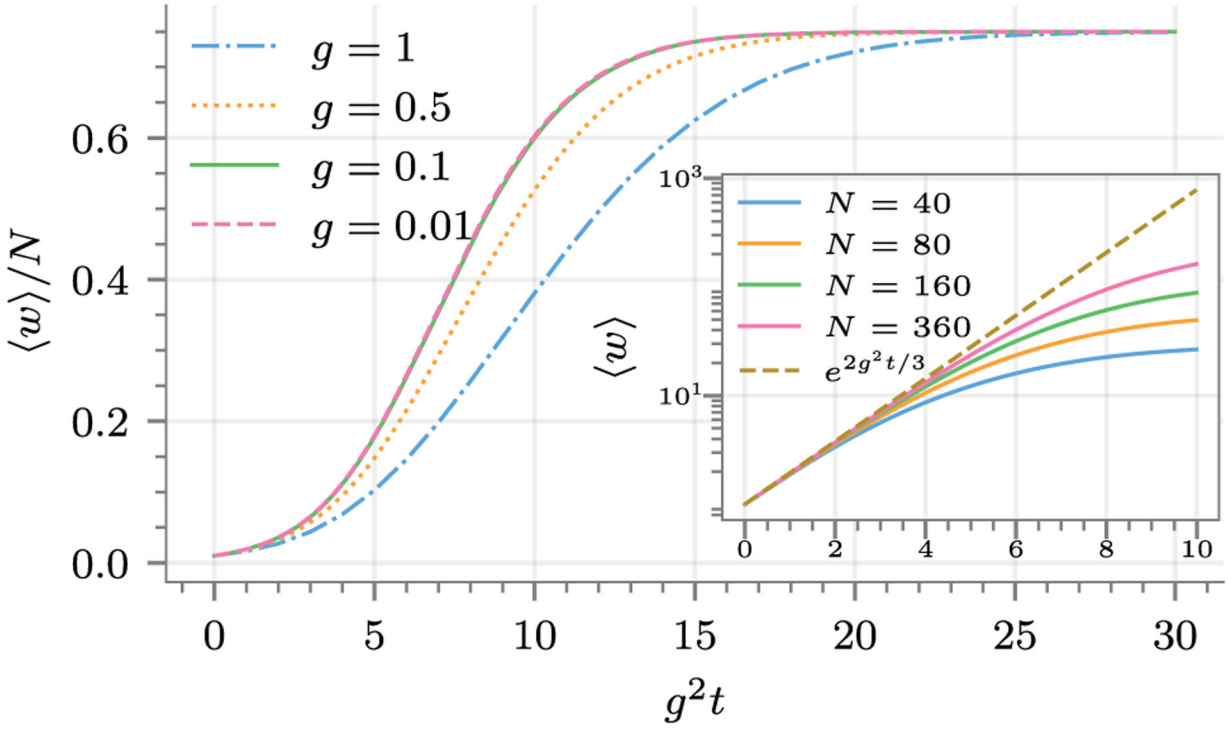

FIG. 2.

Normalized mean operator weight $\langle w(t) \rangle / N = (1/N) \sum_w w h_t(w)$ as a function of time for different g and $N = 100$, computed using Eq. (7). For small enough g, all the curves collapse to a single curve as a function of $g^2 t$, as implied by Eq. (10). The inset shows the initial exponential increase of $\langle w(t) \rangle$ for different system sizes N and $g = 0.1$.

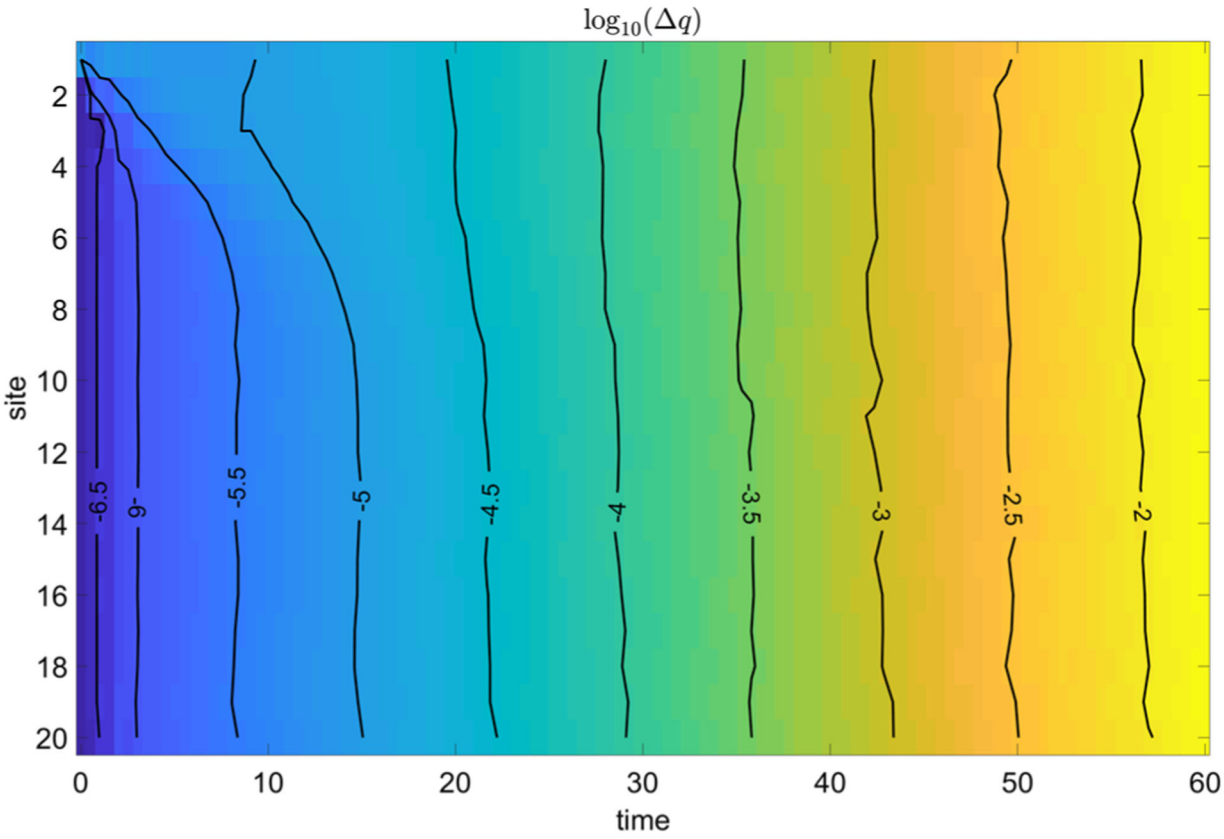

FIG. 3.

$\log_{10} \Delta q_I(t)$ for $N = 20$, $\epsilon = 10^{-5}$, $\Omega_1 = \Omega_2 = 1$, and $\Omega_3 = 2$. The labeled black lines are contours of constant $\log_{10} \Delta q$. Early time ballistic growth is visible in the upper left corner while at later times the system exhibits spatially uniform exponential growth in time.

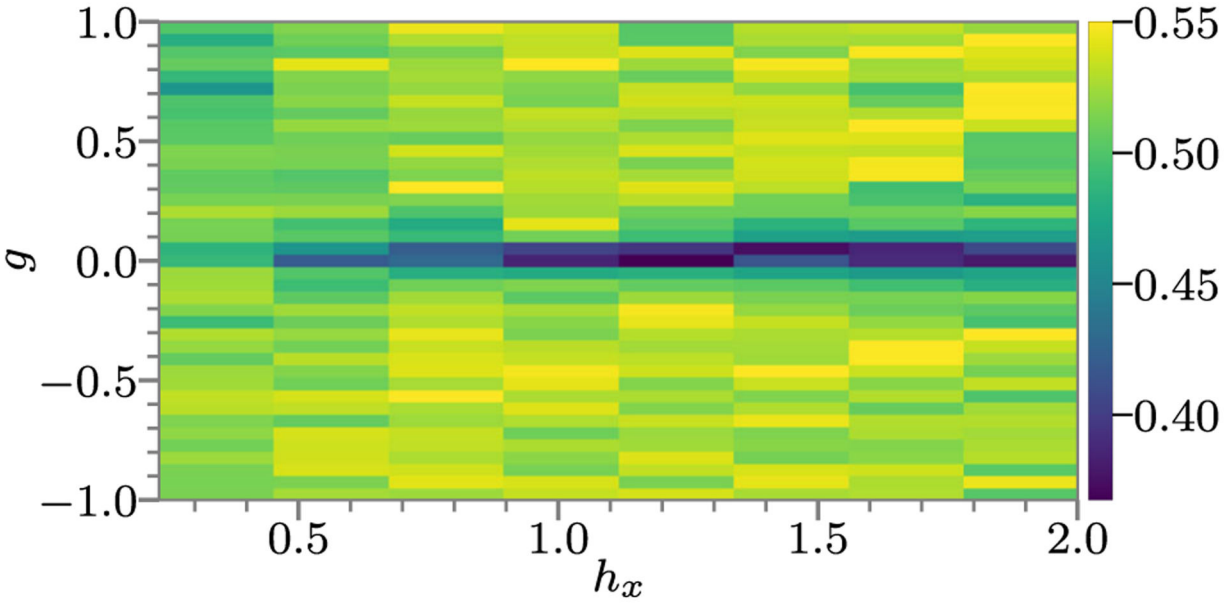

FIG. 4.

Average adjacent-level-spacing ratio $\langle r \rangle$ for the model in Eq. (17) with $J = 1$. Data corresponds to a system of $N = 15$ spins with periodic boundary conditions for fixed momentum and Z-reflection symmetry blocks of the Hamiltonian.

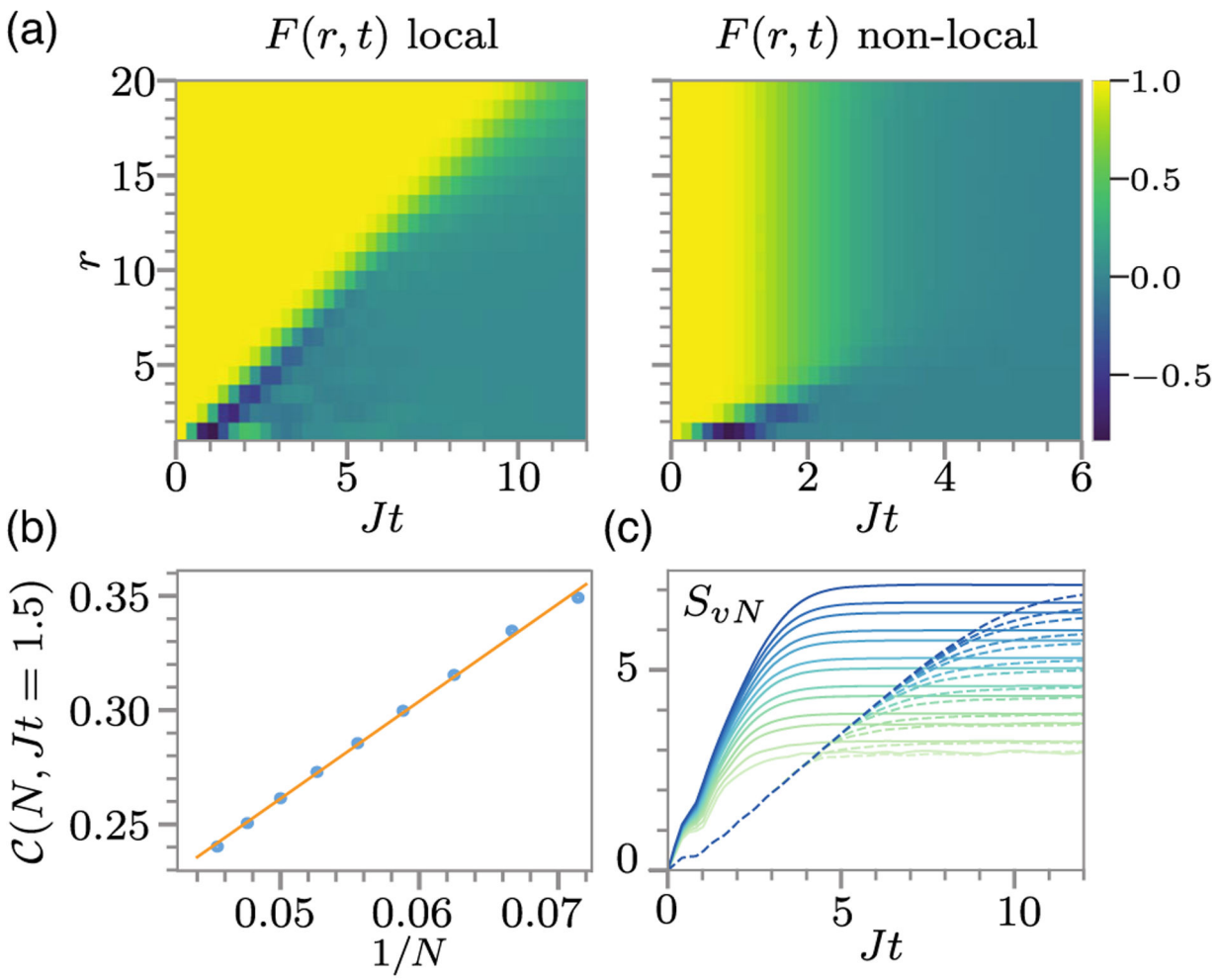

FIG. 5.

(a) Time evolution of the OTOC for the (left) local and (right) nonlocal models. (b) $1 - F(N, t)$ after a fixed evolution time for the nonlocal model (for different system sizes N), showing a linear dependence on $1/N$. The orange line is a linear fit. (c) Half-cut entanglement-entropy growth starting from the $+\hat{\mathbf{y}}$ state for local (dashed lines) and nonlocal (solid lines) models. The color indicates the system size, starting from $N = 10$ (light green) until $N = 22$ (dark blue). For all plots, $J = 1$, $h_x = 1.05$, and $h_z = 0.5$, $g = 0$ ($h_z = 0$, $g = -1$) for the local (nonlocal) models.